SYNTHESIS OF GOLD NANORODS USING THE SEED MEDIATED METHOD AND ITS CONJUGATION WITH ANTIBODY FOR DIAGNOSTIC APPLICATIONS

TEOH POAY LING

UNIVERSITI SAINS MALAYSIA

2012

SYNTHESIS OF GOLD NANORODS USING THE SEED MEDIATED METHOD AND ITS CONJUGATION WITH ANTIBODY FOR DIAGNOSTIC APPLICATIONS

by

TEOH POAY LING

Thesis submitted in fulfillment of the requirements
for the degree of
Master of Science

February 2012

DECLARATION

I hereby declare that I have conducted, completed the research work and written the dissertation entitled “Synthesis of gold nanorods using the seed mediated method and its conjugation with antibody for diagnostic application”. I also declare that it has not been previously submitted for the award of any degree or diploma or other similar title of this for any other examining body or University.

Name of Student: Teoh Poay Ling Signature:

Date:

Witness by

Supervisor: Dr. Khairunisak Abdul Razak Signature:

Date:

ACKNOWLEDGEMENTS

First of all, I would like to express my sincere gratitude to my supervisor, Dr. Khairunisak Abdul Razak for her guidance, assistance and her patience in this research. I am impressed by her beautiful sharp mind. I also would like to express my honour gratitude to Assoc. Prof. Dr. Shaharum Shamsuddin and Assoc. Prof. Dr. Azlan Abdul Aziz for their guidance and help.

I would like to thank all technicians in School of Materials and Mineral Resources Engineering and INFORMM who helped me a lot especially Ms. Diana, Madam Fong and Mr. Mohd. Azrul. Besides, I would like to express my appreciation to my best friends Mr. Navan, Ms. Rabizah, Ms. Hajarul, Ms. Shimah, Ms. Syafinaz, Ms. Ng Soo Ai, Ms. Ng Chai Yan for sharing my laughs and tears. Befriends with all of you is the most beautiful parts of my life at School of Materials and Mineral Resources Engineering and INFORMM. Also I would like to thank Universiti Sains Malaysia for awarding me with USM Fellowship, which covers my living expenses and tuition fees during two years of research. Finally, I would like to express my deepest gratitude to my family for providing constant moral support and encouragement.

Thank you.

TABLE OF CONTENTS

		Page
TITLE		i
DECLARATION		ii
ACKNOWLEDGEMENTS		iii
TABLE OF CONTENTS		iv
LIST OF TABLES		viii
LIST OF FIGURES		x
LIST OF ABBREVIATIONS		xviii
LIST OF SYMBOLS		xx
ABSTRAK		xxi
ABSTRACT		xxii
CHAPTER 1: INTRODUCTION		
1.1	Research background	1
1.2	Problem statement	4
1.3	Objectives	6
1.4	Overview of thesis	6
CHAPTER 2: LITERATURE REVIEW		
2.1	Introduction	8
2.2	Brief history of gold nanoparticles (AuNPs)	8
2.3	Definition and background studies of gold nanoparticles (AuNPs)	9
2.4	Optical properties: Surface plasmon resonance (SPR) in gold nanoparticles (AuNPs)	16
2.5	Synthesis methods to produce gold nanoparticles (AuNPs)	22
	2.5.1 Gold nanospheres (AuNSs)	23
	2.5.2 Gold nanorods (AuNRs)	36

2.5.2.1 Synthesis parameters 40
(a) Effect of surfactant 40
(b) Effect of silver 46
(c) Effect of synthesis temperature 49
2.6 Shape separation of colloidal gold nanorods (AuNRs) 52
2.7 Stability of colloidal gold 55
2.7.1 Critical coagulation concentration (CCC) 56
2.7.2 Electrostatic stabilization 58
2.7.3 Polymeric stabilization 59
2.8 Antibodies 61
2.9 Bioconjugation strategies 67
2.10 Applications of gold nanoparticles (AuNPs) 74
2.10.1 Diagnostic applications 74
(i) Biosensor application 75
(ii) Imaging application 80
2.10.2 Therapeutics applications 82
(i) Photothermal therapy 82
(ii) Drug delivery system 85

CHAPTER 3: METHODOLOGY

3.1 Introduction 87
3.2 Experimental Procedures 88
3.2.1 Synthesis of gold nanoparticles (AuNPs) using stepwise citrate seed mediated growth method 88
3.2.2 Synthesis of gold nanoparticles (AuNPs) using CTAB capped seed mediated growth method 91
3.2.2 (a) Preparation of seed solution 91
3.2.2 (b) Preparation of growth solution 91
3.3 Gold nanorods (AuNRs) PEGylation 93
3.4 Preparation of SH groups containing mouse anti-human IgG_4 (DL- 94

dithiothreitol (DTT) reduction method)
3.5 Optimization for production of reduced mouse anti-human IgG_4 95
3.5.1 Sodium dodecyl sulphate-polyacrylamide gel electrophoresis (SDS PAGE) 95
3.5.2 Silver staining of SDS-PAGE gel 97
3.5.3 Molecular weight estimation of reduced mouse anti-human IgG_4 using SDS-PAGE 98
3.6 Direct conjugation of gold nanorods (AuNRs) to mouse anti-human IgG_4 and reduced mouse anti-human IgG_4 99
3.7 Covalent attachment between gold naorods (AuNRs) with reduced mouse anti-human IgG_4 100
3.8 Characterization for conjugation of AuNRs with mouse anti-human IgG_4 102
3.8.1 ICG strip assay or lateral-flow assay procedure 102
3.9 Samples characterization 104
3.9.1 Transmission electron microscopy (TEM) analysis 105
3.9.2 Ultraviolet-Visible near-infrared spectrophotometer (UV-Visible NIR spectrophotometer) 105
3.9.3 X-ray powder diffraction (XRD) 106

CHAPTER 4: RESULTS AND DISCUSSION

4.1 Introduction 107
4.2 Citrate seed mediated growth method 108
4.2.1 Effect of silver nitrate ($AgNO_3$) concentration 111
4.2.2 Effect of CTAB concentration 118
4.2.3 Effect of volume of seed solution 123
4.3 CTAB seed mediated growth method 126
4.3.1 Effect of CTAB concentration 128

4.3.2 Effect of volume of seed solution 137

4.3.3 Effect of ascorbic acid concentration 145

4.3.4 Effect of nitric acid volume 153

4.4 Stability of the AuNRs 163

4.5 Conjugation of gold nanorods (AuNRs) with mouse anti-human IgG_4 165

4.5.1 Gold nanorods (AuNRs) PEGylation 168

4.5.2 SMCC-Based conjugation 170

4.5.3 Molecular weight estimation of reduced mouse anti-human IgG_4 by using sodium dodecyl sulphate-polyacrylamide gel electrophoresis (SDS-PAGE) analysis 171

4.5.4 Development and optimization of the immunochromatrographic (ICG) strip assay 174

(a) Mouse anti-human IgG_4 conjugated to AuNRs 174

(b) Reduced mouse anti-human IgG_4 conjugated to AuNRs 179

(c) Reduced mouse anti-human IgG_4 covalently conjugated to AuNRs using a SMCC crosslinker 182

4.5.5 Determination of test results with positive and negative serum 184

CHAPTER 5: CONCLUSIONS AND RECOMMENDATION

5.1 Conclusions 187

5.2 Recommendation for future work 188

REFERENCES 190

APPENDICES

LIST OF TABLES

		Page
Table 2.1:	Methods to synthesize AuNPs	13
Table 2.2:	Size and shape determine the physical colour of AuNPs	19
Table 2.3:	Plasmon mode of the AuNPs with varying shapes	21
Table 2.4:	Reducing agents in synthesizing AuNSs	24
Table 2.5:	Particles size, plasmon band maximum and size distribution synthesized with stepwise and one step of seeding growth method	34
Table 2.6:	Methods to produce AuNRs	40
Table 2.7:	List of growth reaction using different supplier CTAB	42
Table 2.8:	Summary of AuNRs with synthesis temperature	50
Table 2.9:	The size of mother sol and after sample centrifugation	54
Table 2.10:	The crosslinker reagents for coupling protein to nanoparticles	68
Table 2.11:	Reported LOD and assay time for gold labeling in immunochromatographic strip assay	78
Table 3.1:	The amount of all parameters to synthesize AuNPs	90
Table 3.2:	Summary of the effect of parameter study	93
Table 4.1:	Dimension of gold nanorods (AuNRs) and bipyramids (BPs) at Step B	116
Table 4.2:	Aspect ratio of gold nanorods (AuNRs) and bipyramids (BPs)	122
Table 4.3:	Physical properties of AuNRs with varying CTAB concentration; transverse surface plasmon (TSP), longitudinal surface plasmon (LSP) position, length, diameter and aspect ratio	133
Table 4.4:	Physical properties of AuNRs with varying volume of seed solution; transverse surface plasmon (TSP), longitudinal surface plasmon (LSP) position, length, diameter and aspect ratio	142

Table 4.5:	Physical properties of AuNRs with varying ascorbic acid concentration; transverse surface plasmon (TSP), longitudinal surface plasmon (LSP) position, length, diameter and aspect ratio	150
Table 4.6:	Physical properties of AuNRs with varying volume of nitric acid; transverse surface plasmon (TSP), longitudinal surface plasmon (LSP) position, length, diameter and aspect ratio	160
Table 4.7:	Physical properties of AuNRs PEGylation with varying volume of PEG-amine; transverse surface plasmon (TSP), longitudinal surface plasmon (LSP) position	170
Table 4.8:	The distinct fragments of mouse anti-human IgG_4 antibody after reducing by DTT	173
Table 4.9:	Values of absorbance and plasmon locations of AuNRs and AuNRs directly conjugated to mouse anti-human IgG_4	177
Table 4.10:	Values of absorbance and plasmon locations of AuNRs and AuNRs directly conjugated to reduced mouse anti-human IgG_4	180
Table 4.11:	Values of absorbance and plasmon locations of AuNRs and AuNRs covalently conjugated to reduced mouse anti-human IgG_4	183

LIST OF FIGURES

Figure 2.1:	SPR occurs when the interaction between electromagnetic (EM) field with the electrons in the conduction band for a metal sphere	17
Figure 2.2:	Optical absorption spectra of AuNRs with different aspect ratios: (a) 2.4; (b) 3.0; (c) 3.9; (d) 4.8; (e) 5.6	18
Figure 2.3:	Photograph of five of AuNRs solution. Aspect ratios are (a) 1.7, (b) 2.3, (c) 2.7, (d) 3.5 and (e) 4.0 (from the left to right)	20
Figure 2.4:	The color of AuNRs solution of having different amount of spheres as byproduct. (a) 50%, (b) 30%, (c) 10%, and (d) 0%	20
Figure 2.5:	Schematic illustration of plasmon resonance of solid metal, (A) gold nanoparticle, (B) nanorod, (C) hollow gold nanospheres (HGN), and (D) aggregate gold nanoparticles	22
Figure 2.6:	Transmission electron microscopy images of $Na_3Ct/HAuCl_4$ molar ratio from 0.7:1 to 17.5:1 ((a)-(e)), (f) average size AuNPs synthesis with different $Na_3Ct/HAuCl_4$ molar ratio	27
Figure 2.7:	Predictions of dependence of particle size on the ratio of citric acids to gold for fixed value of $[T_0] = 3 \text{ X } 10^{-4}$ M	29
Figure 2.8:	Mechanism of growth and agglomeration of AuNSs synthesized with varying pH, (a) $pH < 5.0$, (b) $5.9 < pH < 7.2$, and (c) $pH > 9.1$	30
Figure 2.9:	Transmission electron micrographs of AuNPs obtained by citrate reduction at the different pH values	31
Figure 2.10:	TEM images of AuNSs grown with seeding growth method: (a) 50 nm, (b) 78 nm, (c) 105 nm, and (d) 143 nm	34
Figure 2.11:	An AuNRs created by CTAB bilayer. The black circles represent ammonium head groups while the yellow zig zag represents hydrocarbon tail of CTAB	41
Figure 2.12:	TEM (top images labeled with "1") and SEM (bottom images labeled with "2") images of AuNPs with CTAB from five different suppliers: (A) Fluka (52370) (B) MP Biomedicals (C) Acros (D) Sigma (H5882) and (E) Aldrich. Only CTAB supplied	43

by Fluka and MP Biomedicals yielded nanorods, while the others yielded only spherical particles

Figure 2.13: TEM micrographs of AuNPs prepared in the presence of (a) C_{10}TAB, (b) C_{12}TAB, (c) C_{14}TAB, and (d)C_{16}TAB 44

Figure 2.14: XRD pattern of AuNRs prepared using seed mediated growth method 45

Figure 2.15: Influence of the type of surfactant used in growth solution on the morphology of the AuNRs:, (a) CTAB, (b) CTAC and (c) CTAB + BDAC. The scale bar is 50 nm 46

Figure 2.16: An underpotential deposition (UPD) of silver atom on Au {111}, {100}, and {110} facets 47

Figure 2.17: (a) High-Resolution TEM image of citrate seeds and (b) TEM image of gold nanostructures grown from citrate seeds with silver 49

Figure 2.18: (a) High-Resolution TEM image of CTAB seed and (b) TEM image of AuNRs grown from CTAB seeds with silver 49

Figure 2.19: TEM images of nine samples prepared at: (a) 2.5 ℃, (b) 10 ℃, (c) 15 ℃, (d) 20 ℃ (e) 25 ℃, (f) 55 ℃, (g) 80 ℃ and (h) 95 ℃. The scale bar is 500 nm for images a-d, 100 nm for images e, g and h, and 50 nm for image f 50

Figure 2.20: Evolution of the integrated absorbance vs time for AuNRs synthesized at different temperatures 52

Figure 2.21: UV-Vis-NIR spectrum of (a) mother colloidal sol and (b) separated sols deposited on the side wall and deposit at the bottom of tube 53

Figure 2.22: Figure 2.22: TEM images of AuNRs: (a) before centrifuge, (b) after centrifuge-nanorods deposited at the side of the centrifuge tube and (c) after centrifuge-sediment deposited at the bottom of the centrifuge tube 53

Figure 2.23: UV-Vis-NIR spectra for the CTAB series at (a) 100 mM, (b) 1mM and (c) 0.5 mM 55

Figure 2.24: Time resolved absorption spectra of AuNRs in the presence of NaCl with a certain concentration of (a) 0.86 M and (b) 2.58 M 57

Figure 2.25: Effect of polymer chains on the colloidal dispersion 60

Figure 2.26:	Structure of antibody	62
Figure 2.27:	Separation of IgG antibodies into fragments using SDS-PAGE, (a) lane 1-4: IgG treated with DTT, lane 5-8: different amount IgG without DTT, (b) different amount of IgG reduced by DTT	66
Figure 2.28:	SDS-PAGE results of anti-CEA antibody reduction using TCEP (reducing agent) concentration of 0x, 3x, 10x and 30x over the concentration of the antibody	67
Figure 2.29:	EDC reacts with carboxylic acids to create an active-ester intermediate. In the presence of an amine nucleophile, an amide bond is formed with release of an isourea by-product	70
Figure 2.30:	Maleimide coupling of an amine (NH_2) group and thiol (SH) group using SMCC as a linker	73
Figure 2.31:	Classification of the diagnostic applications of AuNPs	75
Figure 2.32:	Immunochromatographic strip test device	78
Figure 2.33:	Diagnostic tool for meningococcal diagnostic test	80
Figure 2.34:	Various applications of gold nanoparticles (AuNPs) in therapy application	82
Figure 2.35:	Synthesis of MMP-AuNR for simultaneous imaging and photothermal therapy	84
Figure 3.1:	Flow chart of the AuNPs synthesis route	89
Figure 3.2:	The Amicon Ultra-0.5 product includes 5 different cutoffs	95
Figure 3.3:	Broad range protein molecular weight markers	98
Figure 3.4:	The structure of SMCC	101
Figure 3.5:	Schematic diagram of ICG strip assay	102
Figure 3.6:	Schematic diagram of analyzing ICG strip assay performance after tested with serum. C = control line, T = test line	104
Figure 4.1:	Representation of citrate seed mediated growth for AuNPs	110
Figure 4.2:	(a) TEM images of the citrate seeds grown in aqueous solution and (b) UV-Vis spectra of citrate seeds.	111

Figure 4.3:	UV-Vis-NIR spectra of gold products synthesized by varying $AgNO_3$ concentration. CTAB concentration and seed solution were fixed to 0.2 M and 2 ml, (a) Step A, (b) Step B, and (c) Step C	113
Figure 4.4:	TEM images of gold products synthesized under Step B condition by varying $AgNO_3$ concentration. CTAB concentration and seed solution fixed at 0.2 M and 2 ml respectively: (a) 0.004 M $AgNO_3$, (b) 0.007 M $AgNO_3$, (c) 0.010 M $AgNO_3$, and (d) 0.015 M $AgNO_3$	115
Figure 4.5:	TEM images of gold products synthesized under Step C condition with CTAB concentration and seed solution fixed to 0.2 M and 2 ml, respectively: (a) 0.007 M $AgNO_3$, and (b) 0.015 M $AgNO_3$	116
Figure 4.6:	Shaped evolution for synthesizing of the AuNPs under desired silver nitrate concentration at Step B and Step C with CTAB concentration and seed solution were fixed to 0.2 M and 2 ml respectively	117
Figure 4.7:	UV-Vis-NIR spectra of gold products synthesized with varying CTAB concentration by fixing the $AgNO_3$ concentration at 0.004 M and 2 ml seed solution at: (a) Step A, and (b) Step B	119
Figure 4.8:	TEM images of gold products synthesized under Step B condition with varying CTAB concentration by fixing the $AgNO_3$ concentration at 0.004 M and 2 ml seed solution was used, (a) 0.1 M, (b) 0.2 M and (c) 0.3 M	121
Figure 4.9:	Shapes evolution for synthesizing of the AuNPs under desired CTAB concentration at Step B by fixing the $AgNO_3$ concentration at 0.004 M and 2 ml seed solution was used	122
Figure 4.10:	UV-Vis-NIR spectra of gold products synthesized with varying volume of seed solution by fixing the $AgNO_3$ concentration at 0.004 M and CTAB concentration at 0.2 M at: (a) Step A, and (b) Step B	123
Figure 4.11:	TEM images of gold products synthesized under Step B condition with varying volume of seed solution by fixing the $AgNO_3$ concentration at 0.004 M and CTAB concentration at 0.2 M, (a) 1.1 ml, (b) 1.5 ml, (c) 2.0 ml, and (d) 2.5 ml	125
Figure 4.12:	Shaped evolution for synthesizing AuNPs under desired volume	126

of seed solution at Step B by fixing the $AgNO_3$ concentration at 0.004 M and 0.2 M CTAB

Figure 4.13: Photography of CTAB seed prepared in deionized water after 2 hours 127

Figure 4.14: (a) TEM images of the CTAB seeds grown in aqueous solution and (b) particles size distributions of CTAB seeds 128

Figure 4.15: UV-Vis-NIR spectra of the AuNRs solution with varying CTAB concentration 129

Figure 4.16: TEM images of the AuNRs with varying CTAB concentrations; (a) 0.10 M, (b) 0.15 M, (c) 0.20 M, and (d) 0.30 M 131

Figure 4.17: Histograms for distribution of diameter of AuNRs: (a) 0.10 M, (b) 0.15 M, (c) 0.20 M, and (d) 0.30 M CTAB and length of AuNRs: (e) 0.10 M, (f) 0.15 M, (g) 0.20 M, and (h) 0.30 M CTAB. 132

Figure 4.18: The trend of (a) transverse and longitudinal surface plasmon of AuNRs, (a) length and diameter of AuNRs and (c) aspect ratio of AuNRs with varying CTAB concentration 135

Figure 4.19: XRD patterns of AuNRs with effect of CTAB concentration; (a) 0.10 M, (b) 0.15 M, (c) 0.20 M, and (d) 0.30 M 137

Figure 4.20: UV-Vis-NIR spectra of the AuNRs s solution with varying 10 µl until 70 µl seed solution 138

Figure 4.21: TEM images of the AuNRs at various volume of seed solution (a) 10 µl, (b) 30 µl, (c) 50 µl, and (d) 70 µl 140

Figure 4.22: Histograms for distribution of diameter of AuNRs: (a) 10 µl, (b) 30 µl, (c) 50 µl, and (d) 70 µl seed solution and length of AuNRs: (e) 10 µl, (f) 30 µl, (g) 50 µl, and (h) 70 µl seed solution. 141

Figure 4.23: The trend of (a) transverse and longitudinal surface plasmon of AuNRs, (b) length and diameter of AuNRs and (c) aspect ratio of AuNRs with volume of seed solution 143

Figure 4.24: XRD patterns of AuNRs with effect of volume of seed solution by fixing the CTAB concentration to 0.20 M and ascorbic acid concentration of 0.08 M; (a)10 µl, (b) 30 µl, (c) 50 µl, and (d) 70 µl 145

Figure 4.25:	UV-Vis-NIR spectra of the AuNRs solution with the addition of 0.07 M until 0.10 M ascorbic acid (AA) with CTAB concentration was fixed to 0.20 M and 50 µl seed solution was used	147
Figure 4.26:	TEM images of the AuNRs at various ascorbic acid concentrations at (a) 0.07 M, (b) 0.08 M, (c) 0.09 M, and (d) 0.10 M	148
Figure 4.27:	Histograms for distribution of diameter of AuNRs: (a) 0.07 M, (b) 0.08 M, (c) 0.09 M, and (d) 0.10 M ascorbic acid and length of AuNRs: (e) 0.07 M, (f) 0.08 M, (g) 0.09 M, and (h) 0.10 M ascorbic acid.	149
Figure 4.28:	The trend of (a) transverse and longitudinal surface plasmon of AuNRs, (b) length and diameter of AuNRs and (c) aspect ratio of AuNRs with varying ascorbic acid concentration	151
Figure 4.29:	XRD patterns of AuNRs with effect of ascorbic acid concentrations with CTAB concentration were fixed to 0.20 M and 50 µl seed solution were used; (a) 0.07 M, (b) 0.08 M, (c) 0.09 M, and (d) 0.10 M	153
Figure 4.30:	UV-Vis-NIR spectra of the AuNRs solution with varying volume of HNO_3 with CTAB concentration was fixed to 0.20 M, 50 µl seed solution was used and ascorbic acid was fixed to 0.08 M	155
Figure 4.31:	TEM images of AuNRs synthesized using different volume of HNO_3 with CTAB concentration was fixed to 0.20 M, 50 µl seed solution was used and ascorbic acid was fixed to 0.08 M; (a) 0 µl, (b) 100 µl, (c) 200 µl, (d) 300 µl, (e) 400 µl, and (f) 600 µl	156
Figure 4.32:	Histograms for distribution of diameter of AuNRs: (a) 100 µl, (b) 200 µl, (c) 300 µl, (d) 400 µl, and (e) 600 µl nitric acid and length of AuNRs: (f) 100 µl, (g) 200 µl, (h) 300 µl, (i) 400 µl, and (j) 600 µl nitric acid.	158
Figure 4.33:	The trend of (a) transverse and longitudinal surface plasmon of AuNRs, (b) length and diameter of AuNRs and (c) aspect ratio of AuNRs with volume of HNO_3	161
Figure 4.34:	UV-Vis-NIR spectra of the solution with varying volume of HNO_3 and without $AgNO_3$	162
Figure 4.35:	Mechanism of AuNRs growth from CTAB gold seed	163

nanoparticles in the presence HNO_3 or $AgNO_3$

Figure 4.36: Photographs of colloidal AuNRs. Storage duration is (a) 1 day, (b) 1 week and (c) 4 weeks at room temperature 164

Figure 4.37: UV-Vis-NIR spectra of the AuNRs solution which after 1 day and 4 weeks 164

Figure 4.38: Bioconjugation reaction of AuNRs-amine to free sulhydryl-containing mouse anti-human IgG_4 166

Figure 4.39: Schematic representation of the gold nanorods (AuNRs) PEGylation 169

Figure 4.40: UV-Vis-NIR spectra of the AuNRs solution with varying volume of PEG-amine 169

Figure 4.41: Solutions of conjugation of AuNRs with SMCC. From left to right the SMCC concentration are 0.1 mM, 0.5 mM, 1mM, 2 mM, 4 mM and 5 mM 171

Figure 4.42: Separation of mouse anti-human IgG_4 into fragments using SDS-PAGE analysis. All samples were loaded with 20 μg of mouse anti-human IgG_4. Lane 1-7 is IgG_4 heated at 93˚C prior SDS-PAGE, but different DTT concentration to reduce mouse anti-human IgG_4. From lane 1 to 7 the DTT concentrations are 1 mM, 5 mM, 10 mM, 20 mM, 100 mM, 200 mM and 400 mM, respectively. From lane 8-10, mouse anti-human IgG_4 was treated with 400 mM DTT and heated at 37˚C prior SDS-PAGE at 20 mins, 40 mins and 60 mins 173

Figure 4.43: ICG strip assay using AuNRs directly conjugated to mouse anti-human IgG_4. From left to right are HF 90, HF 135 and HF 240 membrane 175

Figure 4.44: The colloidal AuNRs were challenged with NaCl. Tube 1: 2 μg/ml mouse anti-human IgG_4, Tube 2: 4 μg/ml mouse anti-human IgG_4, Tube 3: 5 μg/ml mouse anti-human IgG_4, Tube 4: 6 μg/ml mouse anti-human IgG_4, Tube 5: 8 μg/ml mouse anti-human IgG_4, Tube 6: 10 μg/ml mouse anti-human IgG_4, Tube 7: 20 μg/ml mouse anti-human IgG_4, Tube C1: 1 ml of AuNRs, and Tube C2: 0.5 ml AuNRs + 0.5 ml NaCl 176

Figure 4.45: UV-Vis-NIR spectra of AuNRs and AuNRs directly conjugated to mouse anti-human IgG_4 177

Figure 4.46:	ICG strip assay using AuNRs directly conjugated to mouse anti-human IgG_4. From left to right the concentration of mouse anti-human IgG_4 are 2, 4, 6, and 8 μg/ml	179
Figure 4.47:	UV-Vis-NIR spectra of AuNRs and AuNRs directly conjugated to reduced mouse anti-human IgG_4	180
Figure 4.48:	ICG strip assay using AuNRs directly conjugated to reduced-IgG_4. From left to right the amount of reduced mouse anti-human IgG_4 are 2, 4, 6, 8 and 10 μl	181
Figure 4.49:	UV-Vis-NIR spectra of AuNRs and AuNRs covalently conjugated to reduced mouse anti-human IgG_4	182
Figure 4.50:	ICG strip assay using AuNRs covalently conjugated to reduced mouse anti-human IgG_4. From left to right the amount of reduced mouse anti-human IgG_4 are 5, 10, 15, 20 and 25 μl	184
Figure 4.51:	ICG strip assay (a) to (c) is test with positive serum result, while test strip (d) to (e) is test with negative serum result. (a) & (d): mouse anti-human IgG_4 directly conjugated to AuNRs, (b) & (e): reduced mouse anti-human IgG_4 conjugated to AuNRs and (c) & (f): mouse anti-human IgG_4 covalently conjugated to AuNRs using a SMCC crosslinker.	186

LIST OF ABBREVIATIONS

Abbreviations	Compound
$AgNO_3$	Silver nitrate
Au	Gold
AuNPs	Gold nanoparticles
AuNSs	Gold nanospheres
AuNRs	Gold nanorods
BSA	Bovine serum albumin
CTAB	Cetyltrimenthylammonium bromide
DI	deionized
DTT	Dithiothreitol
$HAuCl_4$	Gold chloride
HNO_3	Nitric acid
ICG	Immunochromatographic
IgG	Immunoglobulin G
LSP	Longitudinal surface plasmon
$NaBH_4$	sodium borohydride
Na_3Ct	Trisodium citrate
NIR	Near-infrared
PEG	Polyethylene glycol
SMCC	succinimidyl-4-(N-maleimidomethyl)cyclohexana-1-carboxylate
SDS-PAGE	Sodium dodecyl sulfate-polyacrylamide gel electrophoresis

SPR	Surface plasmon resonance
TEM	Transmission electron microscopy
TSP	Transverse surface plasmon
UV-Visible NIR	Ultraviolet-Visible near-infrared
XRD	X-ray powder diffraction

LIST OF SYMBOLS

nm	Nanometer
λ	Wavelength
˚C	Degree celcius
L	Length
D	Diameter
M	Molar
Da	Dalton

SINTESIS NANORODS EMAS MENGGUNAKAN KAEDAH PERANTARA PEMBENIHAN DAN KONJUGAT DENGAN ANTIBODI UNTUK KEGUNAAN DIAGNOSTIK

ABSTRAK

Penyelidikan ini melibatkan sintesis nanorod emas (AuNRs) dengan kaedah perantara pembenihan sitrat dan perantara pembenihan bromida cetyltrimethylammonium (CTAB). AuNRs terkonjugat antibodi adalah untuk kegunaan diagnostik. AuNRs disintesis oleh kaedah perantara pembenihan sitrat melibatkan dua peringkat: pernyediaan larutan benih dan peringkat pertumbuhan. Perbandingan dari segi hasil AuNRs daripada kedua-dua jenis larutan benih, didapati AuNRs yang lebih banyak dan lebih panjang dihasilkan menggunakan benih dari pembenihan CTAB. Sementara itu, ciri-ciri AuNRs juga dipengaruhi oleh parameter sintesis daripada larutan pertumbuhan seperti kepekatan argentum nitrat ($AgNO_3$), kepekatan CTAB, kepekatan asid askorbik, isipadu larutan benih dan isipadu asid nitrik (HNO_3). Di antara sampel ini, parameter sintesis yang optimum untuk menghasilkan AuNRs ialah 0.2 M CTAB, 0.08 M asid askorbik, 50 µl larutan benih dan 300 µl HNO_3 melalui kaedah perantara benih CTAB. Parameter sintesis yang optimum menghasilkan 4.9 nisbah aspek AuNRs. Prestasi AuNRs terkonjugat *mouse anti-human* IgG_4 telah berjaya diuji dengan menggunakan immunokromatografi jalur ujian. Daripada hasil jalur ujian, keamatan garis kawalan bertambah dengan pertambahan jumlah *mouse anti-human* IgG_4. Keputusan ujikaji menunjukkan ikatan kovalen konjugat AuNRs dengan *mouse anti-human* IgG_4 menunjukkan konjugatan yang terbaik.

SYNTHESIS OF GOLD NANORODS USING THE SEED MEDIATED METHOD AND ITS CONJUGATION WITH ANTIBODY FOR DIAGNOSTIC APPLICATIONS

ABSTRACT

This work describes the synthesis of gold nanorods (AuNRs) produced using the citrate seed mediated method and cetyltrimethylammonium bromide (CTAB) seed mediated method. The AuNRs are conjugated with antibody for diagnostic applications. The synthesis of AuNRs via the seed mediated method involves two consecutive stages: preparation of seed solution and growth stage. The AuNRs were formed upon the addition of seed solution into the growth solution. By comparing the yield of AuNRs synthesized from both type of seed solutions, it was found that higher yield and longer AuNRs was produced by using CTAB seed solution. Meanwhile, the properties of AuNRs were also influenced by the synthesis parameters of the growth solution such as concentration of silver nitrate ($AgNO_3$), concentration of CTAB, concentration of ascorbic acid, volume of seed solution and volume of nitric acid (HNO_3). Among these samples, the optimum synthesis parameters to produce AuNRs were 0.2 M CTAB, 0.08 M ascorbic acid, 50 μl seed solution and 300 μl HNO_3 via CTAB seed mediated growth method. The optimum synthesis parameters produced 4.9 aspect ratio of AuNRs. The performance of AuNRs conjugated mouse anti-human IgG_4 was successfully checked using an immunochromatographic (ICG) strip assay. From the test strip result, the intensity of the control line increased with increasing the amount of mouse anti-human IgG_4. The result showed that the covalent attachment between AuNRs and mouse anti-human IgG_4 exhibited the best conjugation.

CHAPTER 1

INTRODUCTION

1.1 Research background

Nanotechnology based approaches have been broadly used in diagnostic applications owing to their high sensitivity, specificity, and abilities. Nanoparticles are recognized as the most common because of its small size in the range of 1-100 nm, which has high surface-to-volume ratio, large surface area, unique electronic and optical properties (Hutchison, 2001; Burda *et al*., 2005; Jongnam *et al*., 2007). With the above characteristics, nanoparticles have been widely used in drug delivery system, cellular imaging and biomedical diagnostic, therapeutic, electrical, biosensor, magnetic, and medical fields (Liu *et al*., 2003; Yu *et al*., 2006; Otsuka *et al*., 2003; Sánchez-Sánchez *et al*., 2010). The well-studied nanoparticles including nanospheres, nanoshells, nanocages, nanorods, gold nanoparticles, quantum dots, paramagnetic nanoparticles, and carbon nanotubes, (Derfus *et al*., 2007; Gao *et al*., 2009; Kam *et al*., 2005; Hirsch *et al*., 2003b; Liao and Hafner, 2005; Skrabalak *et al*., 2007; Liu *et al*., 2007; Sun *et al*., 2008; Zhang *et al*., 2001). There are various methods to synthesize nanoparticles such as photochemistry, radiolysis, reverse micelles, arc discharge, seed-mediated growth, phase transfer reactions, direct reduction method etc (Shon *et al*., 2008; Waere *et al*. 2000; Brust *et al*., 1994; Liu, 2004; Jana *et al*., 2001b; Tang *et al*., 1998).

Of major interest, gold nanoparticles (AuNPs) have gained wide attention in human science. The application of AuNPs has brought the passion of researchers in the information age. AuNPs exhibit excellent optical properties, good physical and chemical properties, chemically stable and nontoxic (Qiao *et al*., 2008; Kim *et al*., 2001; Kumar *et al*., 2008; Daniel and Astruc, 2004; Zhang *et al*., 2001). AuNPs have been used in biomedical imaging, diagnostic tests applications, biochemical sensors, and therapeutics (Robert *et al*., 2006; Jesus *et al*., 2006; Marion *et al*., 2006; Chithrani *et al*., 2006; Hutter *et al*., 2010). The unique physical and chemical properties of AuNPs such as large surface area, availability of versatile chemistry for functionalizing AuNPs surface, and good bio-compaibility of AuNPs make them suitable for conjugation with biological molecules (Zhang *et al*., 2001; Li and Rothberg, 2004; Khalavka *et al*., 2009; Yang *et al*., 2009). Besides, AuNPs can be conjugated with bovine serum albumin (BSA) (Housni *et al*., 2008), peptides (Sun *et al*., 2008), deoxyribonucleic acid (DNA) (Claridge *et al*., 2008), polyvalent nucleic acid (Massich *et al*., 2009), dextran (Aveyard *et al*., 2008) and antibodies (Liu *et al*., 2009; Pasqua *et al*., 2009; Eck *et al*., 2008; Zhang *et al*., 2001; Qiao *et al*., 2008; Kumar *et al*., 2008). Bioconjugation of AuNPs with various biological receptors provides wide range of applications in diagnostic, assembly, biosensor, biodetection, and imaging (Gole *et al*., 2001; Qiao *et al*., 2008; Lee *et al*., 2009; Liu *et al*., 2009, Pissuwan *et al*., 2010a).

Application of AuNPs is dependent on their size and shape such as gold nanospheres (AuNSs) and gold nanorods (AuNRs). The use of AuNPs as imaging agents could provide a promising future in diagnostic applications. Significant diagnostic applications become possible when AuNPs resonances are tuned to the near-infrared wavelength. The optical properties of AuNRs in the near infrared (NIR) make them a good candidate for diagnostic application. The AuNRs have two surface plasmon resonance modes, one longitudinal surface plasmon (LSP) band at 700-1300 nm and one transverse surface plasmon (TSP) band at 520 nm. On the other hand, AuNSs have single surface plasmon resonance mode at 512 nm. The LSP is oscillation of the conduction electrons along the length of the AuNRs and TSP is oscillation of the conduction electrons along the width of the AuNRs. The main advantage of using AuNRs compared to AuNSs in diagnostic application is their strong light absorption and scattering (Chang *et al*., 1997). A few reports proved that AuNRs have shown more than 20-fold sensitivity enhancement in biosensing and 20-times optical absorption efficiencies (Copland *et al*., 2004; Law *et al*., 2009).

In diagnostic applications, the conjugation of AuNRs with antibodies shows combines unique properties of the nanoparticles with the specific and recognition ability of antibodies to antigens. Moreover, conjugation of AuNRs with antibodies also improve the cellular uptake and major intracellular stability (Arruebo *et al*., 2009). The functionalized AuNRs with antibodies (IgG) or other biomolecules enhance detection at any target cell (Joseph and Yu, 2006; Hutter *et al*., 2010).

Besides, Li *et al*. (2005) reported that high aspect ratio of AuNRs exhibited high fluorescence intensity. This unique property of AuNRs finds applications in fluorescent probe microarray assays and optical biosensor application for DNA analysis (Kuemin *et al*., 2011).

1.2 Problem statement

AuNRs have been synthesized by the templating method, photochemical (UV-irradiation) and electrochemical synthesis. Martin (1994) fabricated AuNRs using a hard-template method (electrochemical deposition in a porous membrane). Kim *et al*. (2002) synthesized AuNRs by UV-irradiation using silver ions to control the aspect ratio of AuNRs. However, the aforementioned methods have drawbacks such as producing a large quantity of AuNRs with long reaction time, low processing yield and difficulty in scaling up. These problems can be overcome by using the seed-mediated growth method. The seed mediated growth method is capable of producing high yield AuNRs with simple set up at a shorter reaction time (Park *et al*., 2009; Chen *et al*., 2009). Sau and Murphy (2004) obtained high yielding AuNRs using seed mediated growth method. Jana *et al*. (2004) found that seed mediated growth method can improve monodispersity of nanoparticles with predetermine size by growing large particles from small particles. Gole and Murphy (2004) used ~4 nm AuNPs seeds to grow AuNRs. They reported the seed-mediated growth method can eliminate the nucleation process and promote growth of AuNRs.

Jana *et al*. (2001) used a stepwise citrate seed mediated method whereby low yield AuNRs was formed. Subsequently, Sau and Murphy (2004) modified their approach by replacing the citrate with cetyltrimethylammonium bromide (CTAB) molecules in the seed formation step. The yield of AuNRs was improved but shorter AuNRs were produced. Moreover, some AuNRs produced were in bone-shaped. Nikoobakht and El-Sayed (2003) successfully used CTAB capped seed mediated growth method to synthesize high yield AuNRs with rod shaped nanoparticles. However, their method is difficult in controlling the orientation of the nanorods. Meanwhile, Wu *et al*. (2005) and Bai *et al*. (2009) used three steps CTAB capped seed mediated growth method in the presence of nitric acid (HNO_3). Their method managed to improve the aspect ratio and growth direction of AuNRs. But, three steps growth method is time consuming and requires more chemicals to synthesize the AuNRs. In order to improve the aspect ratio and orientation of the produced AuNRs, the idea of Wu *et al*. (2005) and Bai *et al*. (2009) have been used in this work to improve the research work by Nikoobakht and El-Sayed (2003).

In most works, AuNSs were used as detector reagent in immunochromatographic (ICG) strip assay for visualization of signals because of their stability and easy visual detection attributed to their inherent red color (Nara *et al*., 2010). However, to the authors' knowledge no work has been carried out on using AuNRs as detector reagent in ICG strip assay. In the present work, the ICG strip assay has been used to investigate the performance of AuNRs conjugated to

antibody (mouse anti-human IgG_4). In bio conjugation, the reduced mouse anti-human IgG_4 is more effectively conjugated to the surface positive charge of the CTAB-stabilized AuNRs than unreduced mouse anti-human IgG_4. This is because direct attachment of mouse anti-human IgG_4 to AuNRs surface can result in mouse anti-human IgG_4 inactivity (Jonkheijm *et al*., 2008). Nevertheless, the bioconjugation can be further improved by using covalent attachment between AuNRs with antibody. Covalent attachment may increase antibody stability and the available protein binding (Arruebo et al., 2009).

1.3 Objectives

The main objectives of this research are:

i. To establish the best approach to synthesis gold nanorods (AuNRs).

ii. To obtain optimum conjugation parameters of AuNRs conjugated antibody.

iii. To obtain a prototype of gold conjugated antibody for diagnostic applications.

1.4 Overview of thesis

This dissertation is organized in five chapters. Chapter 1 contains introduction and the objectives of this research. In Chapter 2, literature review which contains definition and background studies of AuNPs, brief history of AuNPs, optical properties of AuNPs and methods to synthesize AuNPs are explained. Also, literature review related to antibodies, coupling strategies for bioconjugation and applications

of AuNPs are discussed. In Chapter 3, experimental procedure, various parameters studied and characterizations techniques are explained. Chapter 4, the outcomes from experiments such as effect of parameters on the growth of AuNRs and effect of AuNRs conjugated to antibodies in diagnostic application are presented. Finally, the conclusion and recommendation for future work are described in Chapter 5.

CHAPTER 2

LITERATURE REVIEW

2.1 Introduction

In this chapter, literature review on background studies, properties, and brief history of gold nanoparticles (AuNPs) are explained. This is followed by a comparison of the various methods used to synthesize AuNPs. Moreover, diagnostic application of AuNPs conjugated with antibody is also discussed.

2.2 Brief history of gold nanoparticles (AuNPs)

AuNPs is one of the most ancient subjects in science. In an antiquity, AuNPs was used for aesthetic and curative purposes. AuNPs have been used to make ruby glass and for coloring ceramics since Glauber's found it in the 17th century of "Purple of Cassius" (Daniel and Astruc, 2004). Around the 1600, Paracelus described the experiment of "aurum potable, oleum auri; Quinta essential auri" with the reduction of auric chloride ($AuCl_3$) and alcoholic extract of plant (Weiser, 1933). But in 18th century, as indicated in a French dictionary, dated 1769, under the heading "or potable", it was mentioned that "drinkable Au contained Au in its elementary form but under extreme sub-division suspended in a liquid" (Chymie, 1769). During Middle Ages, colloidal Au was used to cure various diseases, such as heart and venereal issues, tumors, and for diagnoses syphilis (Brown and Smith, 1980).

In 1857, English scientist Faraday reported the formation of deep-red solution of AuNPs by reduction of an aqueous solution of chloroaurate ($AuCl_4^-$) using phosphorus in CS_2 (a two-phase system). The dried colloidal solution was prepared and the optical properties of thin films were investigated (Faraday, 1857). Faraday's samples of "AuNPs" are still on display at the Royal Institute in London (Peter and John, 2007).The term "colloidal" (derived from the Greek word for glue *kola* (Hayat, 1989), which became the French word *collel* was coined shortly thereafter by Graham, in 1861. Since 1885, colloidal Au has been used for its healing capabilities for the heart and to improve blood circulation. Besides, colloidal gold has been used to heal arthritis since 1927.

In the 20th century, AuNPs have received wide attention because of its importance in the industrial process and biochemistry. AuNPs are expected to be key materials and building blocks as well as play an important role in biomedicine field in the near future (Daniel, 2004; Doty *et al*., 2004; Cushing *et al*., 2004; Love *et al*., 2005; Rosi and Mirkin, 2005).

2.3 Definition and background studies of gold nanoparticles (AuNPs)

Gold nanoparticles (AuNPs) are a cluster of gold atoms with size ranging from 1-100 nanometers. AuNPs have gained increasing importance in nanotechnology due to their special features, such as tunable size and shapes of AuNPs, strong absorption and scattering properties, easy surface functionalization,

biological compatibility, simple set up for synthesizing AuNPs and high stability to oxidation (Sperling *et al*., 2008; Grzelczak *et al*., 2008; Love *et al*., 2005; Kim *et al*., 2004). AuNPs can be synthesized into various shapes such as spheres, rods, wires, ribbons, cubic, triangle and plate. Moreover, the size can be tuned to range between 2 to 500 nm.

The synthesis of colloidal AuNPs via chemical method from a homogeneous solution involves three consecutive stages: nucleation, growth and coagulation. In nucleation stage, nuclei are created upon which growth can occur. During the growth stage, more gold (Au) ions deposit on the existing nuclei and followed by agglomeration of many Au ions onto the growing AuNPs. The latter can occur via the following mechanisms: (i) growth consuming molecular precursors from surrounding solution; (ii) Ostwald ripening or coarsening when larger particles grow at the expense of dissolving smaller ones (Claudi *et al*., 2002; Talapin *et al*., 2001).

AuNPs have received much attention during the past several decades as they play an important role in the various areas of materials sciences. The AuNPs especially gold nanospheres (AuNSs) and gold nanorods (AuNRs) have been widely used in biomedical applications. AuNSs have been produced via numerous techniques including ligand-exchange, phosphine-stabilized, two-phase transfer method, direct reduction method, and seed mediated growth (Luo *et al*., 2005; Waere *et al*., 2000; Shem *et al*., 2009; Brust *et al*., 1994; Turkevitch, 1951; Huang *et al*.,

2007; Patungwasa and Hodk, 2008). Meanwhile, for the synthesis of AuNRs, a number of techniques have been reported such as seed mediated growth, photochemistry and electrochemical method (Nikoobakht and El-Sayed, 2001; Nikoobakht and El-Sayed, 2003; Jana *et al*., 2001b; Gao and Murphy, 2003; Gao and Murphy, 2004; Niu *et al*., 2007; Kim *et al*., 2002; Chang *et al*., 1998). Table 2.1 shows the comparisons of various methods to synthesize AuNPs. According to Luo *et al*. (2005), the ligand exchange method has several limitations in regard to the synthesis of AuNSs such as difficulty in controlling the shell thickness, the number of AuNPs inside each micelle, and the location of nanoparticles. In order to obtain shell nanostructure with one AuNSs per micelle, empty micelles must be separated from the product. Waere *et al*. (2000) used the phosphine-stabilized method to produce AuNSs. This method requires rigorous anaerobic condition and diborane gas as a reducing agent. Diborane gas is a flammable and toxic gas, which is dangerous to the environment and health. Monolayer protected AuNSs synthesized by a two-phase transfer method contain a significant amount of tetraoctylammonium bromide (TOABr) (Water *et al*., 2003). The quaternary ammonium salt of TOABr was used as the phase transfer reagent and as a persistently retained impurity. However, the team is still unclear on the method to confirm the presence of TOABr as an impurity in the nanoparticle samples resulting from the two-phase preparation technique.

Patungwasa and Hodak (2008) have used direct reduction method to produce AuNSs. The size of AuNSs can be easily controlled to form a stable colloidal

suspension. In this approach, Au salt must be heated before citrate addition. Citrate serves as a capping agent because it cannot reduce Au salt at room temperature. However, direct citrate method produced nanospheres with a broad range of size and agglomeration can easily occur. To solve the aforementioned disadvantages, Jana *et al*. (2001b) proposed seed mediated method to produce monodisperse nanospheres. In seed mediated method, smaller AuNSs act as nucleation sites for the growth of larger AuNPs. This method involves two steps preparation of seed solution and growth solution. With this approach, either a one step, or step by step growth can be used to synthesize larger AuNSs. Besides, the AuNRs can also be produced by using seed mediated growth method. The CTAB plays an important role in this approach because CTAB is uniquely suited to produce rod-shape nanoparticles.

Kim *et al*. (2002) developed a method for the synthesis of AuNRs by photochemically reducing Au ions in the presence of CTAB and $AgNO_3$. In that method, an aqueous solution of CTAB, $HAuC1_4.3H_2O$, and $AgNO_3$ was irradiated with UV light. The authors found that the aspect ratio of AuNRs is directly proportional with the amount of $AgNO_3$. In 1997, Yu *et al.* reported the electrochemical method for the aqueous synthesis of AuNRs. In this method metallic Au plate was used as an anode in the electrochemical cell. Meanwhile, the electrolytic solution contains a cationic surfactant, hexadecyltrimethylammonium bromide (C_{16}TAB), and a small amount of tetradodecylammonium bromide ($TC_{12}AB$). There are two main functions of C_{16}TAB in this method,

first as the supporting electrolyte and the second as a stabilizer for nanoparticles to prevent their further growth. The reduction of Au ions from aqueous causes nucleation of AuNRs on the electrode plate. The authors also reported that the presence of silver in the electrolytic solution affect the aspect ratio of AuNRs.

Table 2.1: Methods to synthesize AuNPs.

Method	Description of method	Advantages	Drawbacks	Refs.
(a) Ligand exchange method	Displacement of one ligand for another on AuNSs surface	1. Produce different ligands shells, and AuNPs cluster size can be preserved. 2. Physical properties of ligand shell can be tuned.	1. The shell thickness, the number of AuNPs inside each micelle, and the location of nanoparticles are difficult to control. 2. Empty micelles must be separated from the product to obtain shell nanostructure with one AuNSs per micelle	(Luo *et al*., 2005; Young *et al*., 2008; Tour *et al*., 1995; Brust *et al*., 1995)
(b) Phosphine-stabilized	Using diborane gas to reduce gold chloride ($HAuCl_3$) to form $AuCl(PPh_3)$ under warm benzene	1.Phosphine-stablized particles can act as the starting materials for production of nanoparticles functionalized by other ligands such as thiols, amines, and other phosphines.	1. Requires rigorous anaerobic condition and diborane gas as a reducing agent.	(Shem *et al*., 2009; Feldheim *et al*., 1996; Waere *et al*., 2000)

		2. Phosphine-stabilized nanoparticles are precursors to other functionalized nanoparticle building blocks possesses well-defined metallic core.		
(c) Two-phase transfer	Use stabilizing agent, reducing agent, and tetraoctylammonium bromide (TOABr) to synthesize AuNSs. Reducing agent and TOABr are phase transfer catalyst.	1. Stable and monodisperse nanoparticles can be synthesized.	1. The tetraoctylammonim bromide (TOABr) is always retained even after repeated precipitation and washing with ethanol or acetone. 2. Phase-transfer catalyst is needed during synthesis of AuNPs.	(Rowe *et al*., 2004; Brust *et al*., 1994; Waters *et al*., 2003)
(d) Direct reduction method	The precursor salts, reducing agents and stabilizer are used to synthesis AuNSs.	1. Use less energy. 2. Size of AuNSs can be controlled. 3. Easily form colloidal suspension with high stability. 4. Straight forward to produce nanoparticles.	1. Low yield. 2. Broad size distribution range. 3. Agglomeration easily occurs.	(Turkevitch,1951; Zhu *et al*., 2003; Liu and Philippe, 2004; Huang *et al*., 2007; Patungwasa and Hodak, 2008)
(e) Seed mediated growth	Smaller AuNSs act as nucleation sites for growth of larger	1. Eliminate nucleation step. 2. Promote growth.	1. 1-10 nm nanoparticles are difficult to synthesis 2. Large size distribution	(Jana *et al*., 2001b; Niu *et al*., 2007; Brown and

		AuNSs. This method can also be used to synthesis AuNRs.	3. Improved monodispersity of nanoparticles. 4. Predetermined size of larger particles can be grown from small particles.	range of AuNPs is produced.	Michael, 1998; Brown *et al*., 1999)
(f)	Photo-chemistry	Irradiation of an aqueous solution of gold ions to form AuNRs.	1. Promising for synthesizing uniform nanorods. 2. Reduction of metal ions can be controlled without using excess reducing agent.	1. Long reaction time (more than 30 hours) is required.	(Kim *et al*., 2002; Niidome *et al*. 2003; Dong et al., 2004; Liu and Scaiano, 2009)
(g)	Electro-chemical	Reduction of Au ions from aqueous causes nucleation of AuNRs on the electrode surface. This method has been used to form AuNRs.	1. Holding a good controllability in the particles' dimensions.	1. Low yield of AuNRs.	(Chang *et al*., 1998; Yu *et al*., 1997; Alqudami *et al*., 2008)

AuNPs have been widely used in diagnostic application due to its high stability in biological environment, unique optical properties, large surface area, availability of versatile chemistry for functionalizing AuNPs surface, and excellent biocompatibility (Li and Rothberg, 2004; Davidson and Huang, 2003; Gupta and Velev, 2009; Yang *et al*., 2009). AuNPs are stable in biological environment, thus metallic gold surface can be attached to biomolecules such as antibody, DNA etc with the presence of gold-sulphur bond or electrostatic attraction. Moreover, AuNPs have surface plasmon polaritons and surface plasmon resonances, which are in the visible and near-infrared spectral regions (Hayat, 1989; Schmid, 1992). These properties make AuNPs are sought after in optical imaging and detection applications. Also, gold is a heavy element and has a high atomic number that can be detected by electron microscopes or by X-rays (Gillaspy, 2001).

2.4 Optical properties: surface plasmon resonance (SPR) in gold nanoparticles (AuNPs)

Surface plasmon resonance (SPR) is a quantum optical-electrical phenomenon due to the interaction of incoming light with a metal surface. When the incoming light is larger than the diameter of nanoparticles ($d << \lambda$), the electromagnetic (EM) field across the entire sphere nanoparticle is essentially uniform as shown in Figure 2.1 (Hutter and Fendler, 2004). The free or weakly bound conduction electrons in the noble metal respond collectively when the EM field oscillates back and forth (in the direction of E-field polarization). The resonance is due to the incoming light frequency equal to the intrinsic electron oscillation

frequency. This condition causes the incoming light is completely absorbed. The resonance wavelength is at the position where the maximum light is absorp.

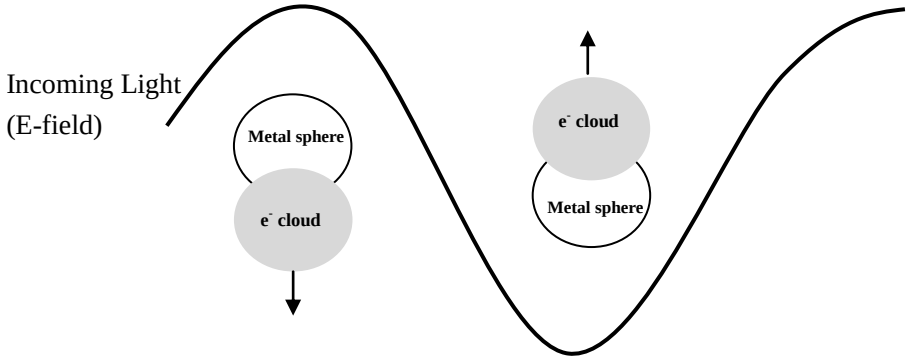

Figure 2.1: SPR occurs when the interaction between electromagnetic (EM) field with the electrons in the conduction band for a metal sphere (Hutter and Fendler, 2004).

AuNRs differ from spheres since they have a particular aspect ratio in which the material is elongated along a single dimension, keeping the other two dimensions approximately equal. It is essential to limit the growth direction to a single axis in order to synthesize nanorods. AuNRs have two peaks in their absorbance spectra that correspond to plasmon resonances: one at approximately 520 nm from plasmon oscillation in the shorter transverse direction and a second at longer wavelength (typically between 700 nm and 1300 nm) from longitudinal oscillation (Burda *et al*., 2005; Brown *et al*., 1999; Link and El-Sayed, 2003). The transverse SPR is due to electronic oscillation across the width of rod shape. Meanwhile, the longitudinal SPR is due to electronic oscillation across the length of the rod shape. By varying the aspect ratio (length divided by width) of rod shape, the position of the longer

wavelength plasmon peak can be tuned out to the near-infrared region, where absorbance by cells and tissue is minimal (Weissleder, 2001). Besides, AuNRs has potential for selective thermal destruction of cancerous tissues (Liao and Hafner, 2005). Figure 2.2 shows adsorption spectra of AuNRs of different aspect ratios. The SPR peaks shift to the right side by increasing the aspect ratio of AuNRs. The color solution of AuNRs are tunable as a function of longitudinal SPR. For short AuNRs with the longitudinal SPR lower than 700 nm, the AuNRs appear in blue color. The deep red color of solution does not change significantly when the longitudinal SPR is between 700 nm and 800 nm. The solution colour changes to pink with the longitudinal SPR larger than 800 nm.

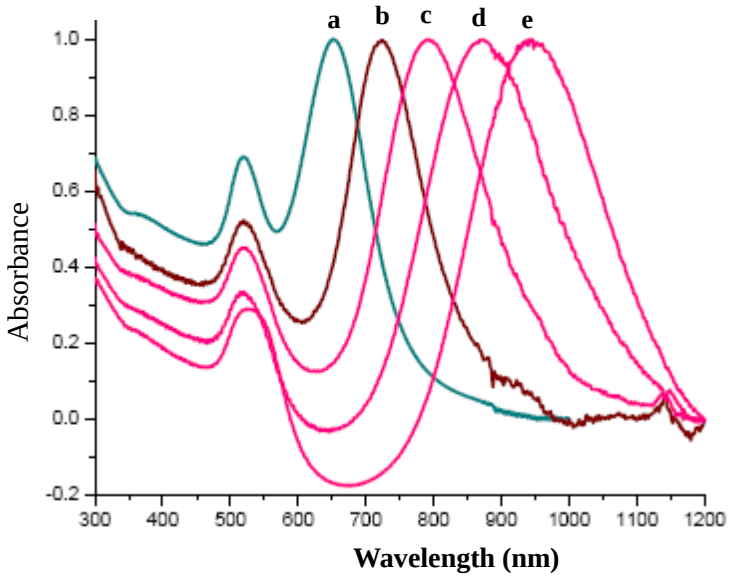

Figure 2.2: Optical absorption spectra of AuNRs with different aspect ratios: (a) 2.4; (b) 3.0; (c) 3.9; (d) 4.8; (e) 5.6 (Huang *et al*., 2009).

The cause of the color dependence is based on the conductive surface's electron vibrational states, called surface plasmon modes. The reflection properties are a dramatic function of the AuNSs diameter. In AuNSs synthesis, the size

influence the colour of the gold colloidal suspension as listed in Table 2.2. The increase of the size of AuNSs causes the color to change from pale blue to violet. This is because increasing the AuNSs size will result in the wavelength of SPR related absorption shifting to longer wavelengths (redder).

Table 2.2: Size and shape determine the physical colour of AuNPs

(Turrkevitch, 1951; Wilenzick *et al*., 1967; Frens, 1973).

Shape	Size in nm	Colour
Spherical	< 3	Pale blue
	12	Pink
	16	Orange
	20-40	Red
	70	Dark magenta
	100-150	Violet

The SPR peaks of AuNRs can be tuned as a function of aspect ratio. Ling *et al*. (2009) produced AuNRs with aspect ratio varying from 1.7 to 4.0, while Park (2006) synthesized AuNRs with further increase in the aspect ratio to 7.4. Figure 2.3 shows the photograph of the AuNRs with aspect ratio varying from 1.7 to 7.4. It can be concluded that the color change could be only observed by human eyes for the AuNRs with aspect ratios below than 3.5. For the AuNRs beyond the aspect ratio of around 3.5, color of the solution is basically the same. That means the color of AuNRs dispersion does not change with further increase in aspect ratio beyond 3.5.

In addition, Park, 2006 found that the color in a visible region is more sensitive to the amount of spherical particles included as byproduct since SPR peak of sphere positions between 500 to 550nm. Figure 2.4 shows the simulated color of

AuNRs with aspect ratio of 5. It can be observed that the color changes from purple to brown as the amount of byproduct decreases from 50 % to 0 %.

Figure 2.3: Photographs of five AuNRs solution. Aspect ratios are (a) 1.7, (b) 2.3, (c) 2.7, (d) 3.5 and (e) 4.0 (from the left to right) (Ling *et al*., 2009; Park, 2006).

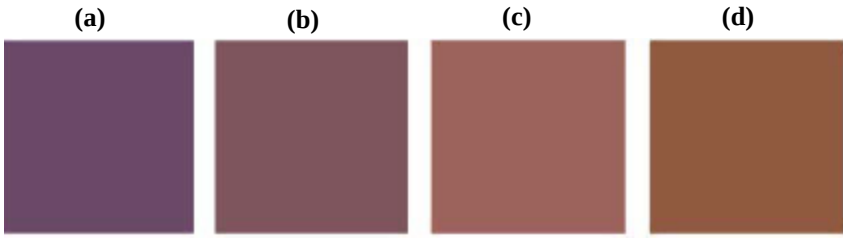

Figure 2.4: The color of AuNRs solution of having different amount of spheres as byproduct. (a) 50%, (b) 30%, (c) 10%, and (d) 0% (Park, 2006).

The free conduction electrons in AuNPs oscillate at specific wavelengths which relate to the nanoparticle's size, and produce an absorbance peak. The SPR absorption peaks of AuNPs can be tuned as a function of particle size, shape, and aggregate morphology (Link *et al*., 1999; Link *et al*., 2004; Kelly *et al*., 2002; Caruso and Antonietti, 2001; Hutter and Fendler, 2004). The size or shape of the

AuNPs alters the electric field density on the surface. This is because the oscillation frequencies of the electrons are changed. Therefore, as the size of the particle increases, the localized surface plasmon dipolar resonance tends to broaden and shift to longer wavelengths. Table 2.3 and Figure 2.5 show the different plasmon modes according to the shape of AuNPs. The spheres and hollow spheres shape only have one plasmon mode, which is called transverse surface plasmon. Meanwhile, rod shape has two plasmon mode called transverse surface plasmon (represent width of AuNPs) and longitudinal surface plasmon (represent length of AuNPs). The aggregates of AuNPs have more complex optical absorption with many bands over a broad spectral region.

Table 2.3: Plasmon mode of the AuNPs with varying shapes.

Shape	Number of plasmon mode	Reason for number of plasmon mode	Refs.
Spheres	1	Completely symmetrical about at perspective	(Encina and Coronado, 2010a; Encina and Coronado, 2010b)
Rods	2	Rod shapes have width and length dimensions	(Zuloaga *et al*., 2010; Grzelczak *et al*., 2007)
Hollow spheres	1 (narrow resonance)	Highly uniform shell structure	(Olson *et al*., 2008; Wheeler *et al*., 2010)
Aggregates	Multiple	Lots of nanoparticles aggregated, many nondegenerate modes arise.	(Schwartzberg *et al*., 2007)

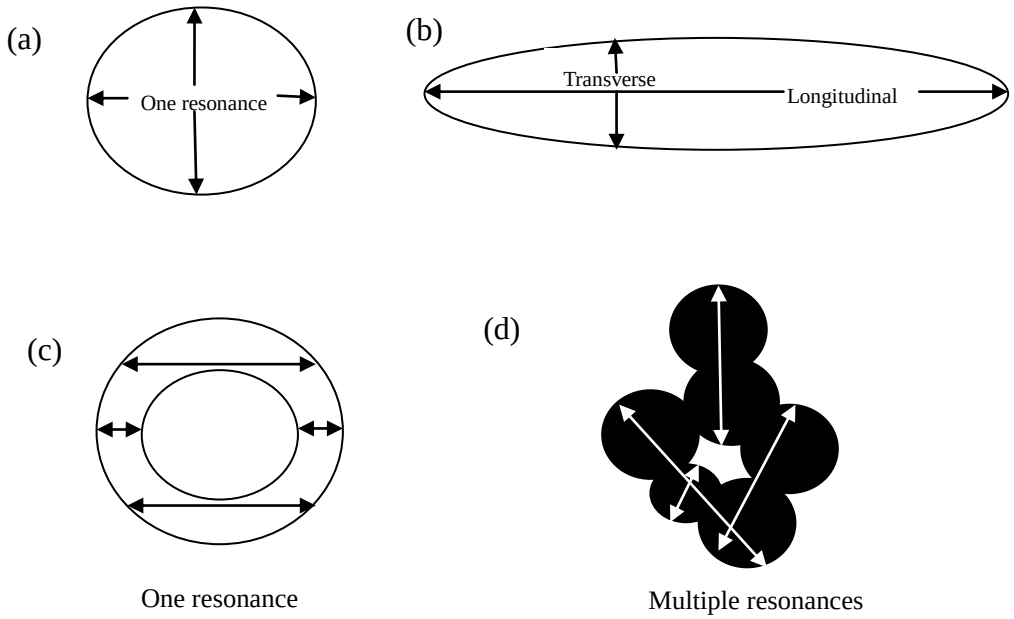

Figure 2.5: Schematic illustration of plasmon resonance of solid metal, (a) gold nanoparticle, (b) nanorod, (c) hollow gold nanospheres (HGN), and (d) aggregate gold nanoparticles (Schwartzberg and Zhang, 2008).

2.5 Synthesis methods to produce gold nanoparticles (AuNPs)

There are various methods to synthesize AuNPs including AuNSs and AuNRs. Among them is wet chemical synthesis method that is cost-effective and has potential for large-scale production of AuNPs. There are two approaches in the synthesis of AuNPs using wet chemical synthesis methods: direct reduction or seed mediated growth method. In direct reduction method, the AuNPs are formed by using reducing agent. Meanwhile, in the seed mediated growth method, firstly small AuNPs are prepared and then used as seeds (nucleation sites) for the preparation of desired size or shape of AuNPs. These seeds will then grow into larger sizes during the growth stage.

2.5.1 Gold nanospheres (AuNSs)

Gold nanospheres (AuNSs) are small spheres which can be in any size from only a few nanometers to several hundred nanospheres (Loo *et al*., 2005). There are two main methods to produce AuNSs by wet chemical synthesis method: direct reduction method and seed mediated growth method. The direct reduction method can be categorized in two ways, (i) Fren method, and (ii) Brust-Schiffrin method. Frens method utilizes citrate reduction of gold salt; AuNSs in the sizes ranging from 12 to 20 nm (relatively size distribution ~10-16 %) can be produced. However, the product has large particles size distribution (polydisperse), tend to aggregate and yields unsatisfactory results (Jana *et al*., 2001b; Brown *et al*., 1999). While in the Brust method, smaller AuNSs (1-5 nm) were synthesized by using sodium borohydride (strong reducing agent) as a reductant.

Direct reduction method is a simple route in synthesizing high quality AuNSs. The advantages of direct reduction method lies in its capability to tune particle size, form a stable colloidal suspension and employ less energy (Turrkevitch, 1951; Zhu *et al*., 2003). The direct reduction method utilizes three main items; a precursor, a reducing agent and a stabilizer. Different chemicals could be used as reducing agents to produce AuNSs. These reagents could be inorganic, organic or natural reducing agent for instance sodium/potassium borohydrate, hydrazine, or organic such as sodium citrate (sometimes known as trisodium citrate), ascorbic acid, soy bean (Chandrasekharan *et al*., 2000; Shukla *et al*., 2008; Tsai *et al*., 2004; Buining *et al*.,

1997; Jana and Murphy, 2001; Kakkassery *et al*., 2004). Table 2.4 summarizes the reducing agents and stabilizers that have been used to synthesize AuNSs. When hydrazine was used as a reducing agent in synthesizing AuNSs, the range of particles size were larger (10-60 nm) compared to when sodium citrate was used (10-22 nm). In addition, the particles size range was 3.5-4.5 nm obtained when trisodium citrate mixed with $NaBH_4$, but the particles size range (17-21 nm) larger when only trisodium citrate was used as reducing agent. The examples of stabilizer are sodium 3-mercaptopropionate (MPA-Na), mercaptosuccinic acid (MSA) etc. Yonezawa and Kunitake (1999) reported that simultaneous addition of sodium 3-mercaptopropionate (MPA-Na) and trisodium citrate can increase the stability of AuNPs. The authors also examined the reduction by a strong reducing agent ($NaBH_4$), but it produced non-uniform MPA-stabilized AuNPs between the ranges of 5 and 20 nm. Zhu *et al*. (2003) reported that MSA is a stronger capping agent than trisodiun citrate. MSA facilitates more uniform and robust capping role in surface-assisted reduction for AuNPs growth.

Table 2.4: Reducing agents in synthesizing AuNSs.

Reducing agent	Stabilizer	Particle size (nm)	Refs.
Sodium citrate	-	10 - 22 nm	(Turrkevitch, 1951; Jana *et al*., 2001a; Kakkassery *et al*., 2004)
Trisodium citrate	Sodium 3-mercaptopropionate (MPA-Na)	2.3 - 10.0 nm	(Yonezawa and Kunitake, 1999)
Trisodium citrate and $NaBH_4$	-	3.5 - 4.5 nm	(Jana *et al*., 2001c)
Trisodium citrate	-	17 - 21 nm	(Zhu *et al*., 2003; Ding *et al*., 2006)
Trisodium citrate	Na_2(MSA)	20.0 nm	(Zhu *et al*., 2003)

Trisodium citrate	Thionine	18.0 nm	(Ding *et al*., 2006)
$NaBH_4$	(γ-mercaptopropyl) Trimethoxysilane (MPS)	1.0 - 5.0 nm	(Buining *et al*., 1997)
$NaBH_4$	Thiol	2.9 - 6.0 nm	(Johnson *et al*., 1998)
$NaBH_4$	Mercaptosuccinic acid (MSA)	1.02 nm	(Chen and Kimura, 1999)
$NaBH_4$	-	2.0 - 2.6 nm	(Maxwell *et al*., 2002)
$NaBH_4$	Thiol or disulfide	1.5 - 3.5 nm	(Maitra & Shreedhar, 2008)
Ascorbic acid	-	5.0 - 50.0 nm	(Wagner and Kohler, 2005; Vemula *et al*., 2006)
Sodium citrate and tannic acid	-	3 - 17 nm	(Tsai *et al*., 2004)
Gallic acid	-	10 - 29 nm	(Wang *et al*., 2007)
Hydrazine	-	10 - 60 nm	(Kawasaki *et al*., 2007)
L-tryptophane	Polyethylene glycol (PEG)	10 - 25 nm	(Akbarzadeh *et al*., 2009)

Among the listed reducing agent, citrate reduction has been widely used. In citrate reduction method, the gold atoms are formed in four reactions (Kumar *et al*., 2007). In reaction (2.1), citrate is initiated with oxidation process and yields dicarboxy acetone. Reaction (2.2) involves reduction of auric salt to form aurous salt. The electrons donated by citrate to gold ions to form gold atoms (Au^0). The aurous salt is regenerated in reaction (2.3), and disproportionation to form gold atoms. The pH of the final solution becomes lower because other ions presence in the medium makes the solution acidic in nature. Reaction (2.4) is the overall stoichiometry of reduction reaction. The reduction of a gold salt ($HAuCl_4$) is to form gold metal. In this reaction, gold can exist in three oxidation states: Au^{3+}, Au^+ and Au^0. Reactions (2.5) and (2.6) show the oxidation energy during the reaction.